JOURNAL OF MATERIALS SCIENCE 20 (1985) 1739–1747

Doping effects on indentation plasticity and fracture in germanium

S. G. ROBERTS, P. PIROUZ, P. B. HIRSCH
Department of Metallurgy and Science of Materials, University of Oxford, UK

Vickers micro-indentation tests have been performed in the temperature range 20 to 420° C on the {0 0 1} surfaces of germanium crystals of three different dopings: "intrinsic", heavily doped p-type and heavily doped n-type. Indentation sizes, dislocation rosette sizes and median/radial crack lengths were measured. Rosette sizes were found to depend strongly on doping, being respectively larger and smaller than in intrinsic material for n-type and p-type specimens, over the temperature range 20 to 420° C. This result correlates well with dislocation velocity measurements in germanium. Indentation size (hardness) was found to vary with doping above ~ 300° C, hardness increasing from n-type through intrinsic to p-type material. Crack lengths, as a function of temperature, showed a sharp transition (to much shorter crack lengths) at a well-defined temperature; this ductile/brittle transition temperature was found to depend on doping, being lowest for n-type (~ 290° C) and highest for p-type (~ 400° C). This is the first observation of a relation between a fracture parameter and bulk electronic doping.

1. Introduction

Dislocation velocities in semiconductors have been known for some time to be dependent on the type and concentration of electrically active dopants [1–3]. Several models have been proposed for this effect [4–8] and these have been critically reviewed by Hirsch [9]. Recently, it has been shown that, in silicon, such doping can alter the value of the lower yield stress [10] and affect the extent of dislocation "rosettes" around microhardness indentations [11]; a model was developed relating the sizes of the rosettes to a minimum stress for motion of the dislocations. The work described here extends these investigations to germanium. This material is of interest for a number of reasons:

1. In silicon, both n- and p-doping were found to increase dislocation velocity with respect to that for intrinsic material. In germanium, n- and p-doping have been shown to have opposite effects on dislocation mobility, the order of increasing mobility being p-doped, intrinsic, n-doped [1, 12].

2. Germanium is more plastic at low temperatures than silicon, allowing experiments to be carried out over a range of temperatures with the low-temperature testing equipment currently available to us.

3. Germanium was found to etch much more easily than silicon, making reliable results more readily obtainable.

As in the experiments on silicon [11], measurements were made of the hardness values and rosette sizes. Also, large changes in cracking behaviour with temperature were observed, and so the crack lengths were measured as a function of temperature, load and doping.

These experiments form part of a wider study aimed at investigating doping effects on the mechanical behaviour of engineering ceramics such as silicon carbide and diamond. For these materials, large single crystals suitable for direct dislocation velocity measurements or compression testing are not easily available, and so indentation-based techniques will be necessary. The tests on silicon and germanium were performed to show the applicability of indentation testing to the investigation of the doping effects, and to correlate data thus obtained with data from compression and bend tests (e.g. [1–3, 10, 12]).

0022–2461/85 $03.00 + .12

2. Experimental methods

2.1. Materials and preparation

Czochralski-grown germanium crystals of three different dopings were used: n-type, arsenic-doped to 5.5×10^{18} cm^{-3}; p-type, gallium-doped to 2.3×10^{19} cm^{-3} and p-type, gallium doped to 3×10^{15} cm^{-3} ("intrinsic"). These will be referred to as N, P and I specimens, respectively. The crystals were oriented by Laue techniques, and slices parallel to {001} were cut using a wire-saw. These slices were lapped, using alumina slurry on cast-iron plates, and polished on diamond-impregnated cloths, finishing with $\frac{1}{4}$ μm diamond. Final polishing, to remove any residual surface damage, was performed using recirculating "Syton" on a soft cloth.

2.2. Indentation testing

Specimens were cleaved to the required size along ⟨110⟩ directions and mounted on a hot-plate on a Matsuzawa MHT1 microhardness tester. In all tests, specimens of all three dopings were indented in the same heating cycle, so as to eliminate any possibility of differences between the specimens arising because of slightly different testing temperatures. Tests were performed using the load range 10 to 200 g, in air, with a dwell time of 15 sec. A Vickers profile diamond indenter was used, with its diagonals parallel to the ⟨110⟩ directions. The indenter was not independently heated, but was positioned over the specimen during the heating cycle so as to minimize the temperature difference between the specimen and the indenter. As in the previous experiments on silicon [11], the specimens were then annealed at the nominal temperature of indentation for 30 min. In this way, the final configuration of the dislocation rosettes is characteristic of the residual indentation stress field at the temperature of indenting/annealing. Tests were made at temperatures in the range 20 to 420° C.

Additionally, a limited number of specimens was indented in a purpose-built hot-hardness tester (Cambridge University Department of Metallurgy and Materials Science). Here, tests were performed at 400 to 500° C, in vacuum, with the indenter heated to the same temperature as the specimen. As well as extending the temperature range of tests above the currently possible on our machine, these tests enabled the effects of using an unheated indenter to be investigated; it appeared that indenting at a nominal 400° C using an unheated indenter roughly corresponded to indenting at ~ 340° C using a heated indenter (see Section 3.1.).

It should be noted that, for the dopings used here, the highest testing temperature approaches the temperature at which the intrinsic carrier density becomes equal to the extrinsic carrier density (~ 500 to 600° C). Thus it might be expected that changes in mechanical properties with doping would be small at the highest temperatures used.

2.3. Etching

Specimens were etched at room temperature in a reagent described by Tuck [13], consisting of 11 cm^3 acetic acid with 30 mg iodine dissolved, 5 cm^3 40% HF and 10 cm^3 HNO_3. A very short etch (1 to 2 sec) was performed first; this accentuated the median/radial cracks, which were then measured. Specimens were then etched for 10 to 20 sec to show dislocation positions.

2.4. Electron microscopy

Some specimens were prepared for transmission electron microscopy (TEM). A grid of 10 g indentations was made so as to cover ~ 1 mm^2 on a specimen cleaved to 2 mm × 3 mm. The specimen was polished until ~ 30 μm thick, and then ion-beam thinned to perforation, polishing and thinning from the unindented side only. Areas around some indentations were then thin enough to be examined in a JEOL JEM100B microscope, where micrographs were taken of the rosettes using two-beam bright-field and centred dark-field illumination conditions.

3. Results

3.1. Hardness measurements

Typical hardness results, in the form of a graph of indentation diagonals at 50 g load, plotted as a function of temperature and doping, are shown in Fig. 1. Similar behaviour was observed at all loads used. Note that, as hardness is inversely proportional to the square of the indentation diagonal, the fractional changes in hardness values will be greater than the fractional changes in indentation diagonal length. Typical hardness values are shown in Table I.

The figure also shows the differences arising from the use of heated and unheated indenters. Extrapolation of the "hot indenter" curve to lower temperatures shows a mismatch between the

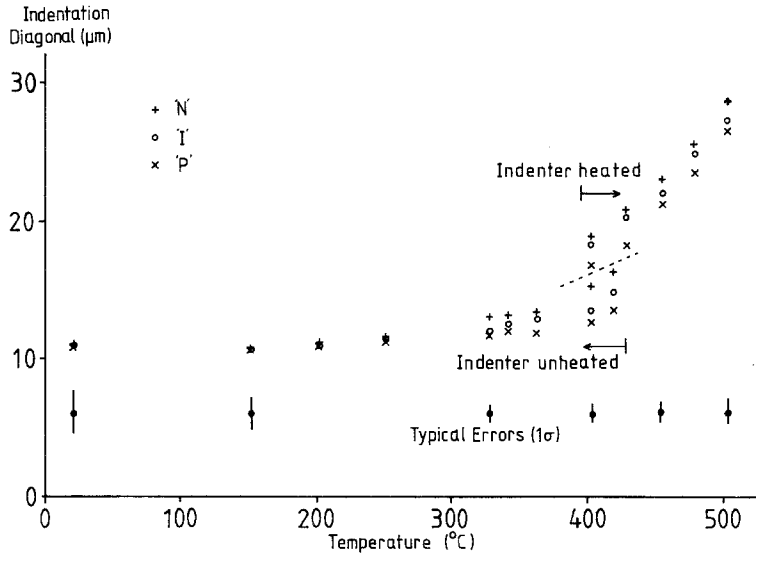

Figure 1 Variation of indentation diagonal size (d) (Vickers indenter, 50 g load) with doping and temperature. Note variation of hardness ($\propto 1/d^2$) with doping in the temperature range ~ 320 to 500° C. N-type material is softest, p-type hardest.

two of ~ 60° C at 400° C. Consequently, there are, in effect, no hardness data for the temperature range 340 to 400° C. However, the general trends are clear for the data available:

1. Hardness values (i.e. indentation diagonal sizes) at low temperatures (less than ~ 300° C) do not depend significantly on doping.

2. Above this temperature, the hardness behaviour of the three types of germanium diverges, p-type being hardest and n-type being softest. The difference in hardness values is greatest at ~ 400° C, using the unheated indenter (see Table I).

3. At temperatures greater than 400° C, the range of diagonal sizes relative to the mean values and thus the range of hardness values relative to the mean values and to the errors in the measurements (see Table I) decrease again until, at 500° C, the hardness values for N, I and P specimens are barely distinguishable.

The hardness/temperature curves shown here follow very closely those previously published by Sumino and Hasegawa [14] for {1 1 1} indentations on near-intrinsic germanium.

TABLE I Hardness of germanium at various temperatures

Type	Temperature (° C)			
	250	400 (cold ind.)	400 (hot ind.)	500
N	684	404	265	112
I	697	520	275	125
P	732	581	334	131
Typical error (2σ)	± 60	± 50	± 40	± 20

Hardness units are kg mm^{-2}; all measurements made at 50 g load.

3.2. Dislocation rosettes

Dislocation half-loops can move out along the {1 1 1} glide planes surrounding the indentation site to form "rosettes". A simplified model of the likely geometry of slip around the indentation is shown in Fig. 2. Prismatic dislocation loops move out from the indentation site on the "V-prisms" formed by intersection of {1 1 1} type planes around the indentation; the dislocations in the same rosette arm all have the same Burgers vector, $\boldsymbol{b} = \frac{1}{2}\langle 1\,1\,0\rangle$. The figure shows the simplest case, with the dislocations being straight and of the 60° type; the shaded area represents extra material in the rosette arm, accommodated as extra half-planes associated with the dislocation loops. The dislocations would be expected to be dissociated into Shockley partials on the glide planes.

Fig. 3 shows bright-field TEM images, using 2 2 0 reflections, of dislocation arrays on one side of a rosette arm. Using the diffracting conditions in Fig. 3a, both Shockley partial dislocations of the type 1/6 ⟨2 1 1⟩ would be in contrast and an array of dislocations of one or both types can be seen. The image in Fig. 3b is characteristic of contrast from overlapping stacking faults of type 1/3 ⟨1 1 1⟩. At this stage it is not known whether these faults are bounded by two types of partials whose equilibrium separation is abnormally wide (as observed in specimens compressed at low temperature and high stress [10, 15]), or whether, at

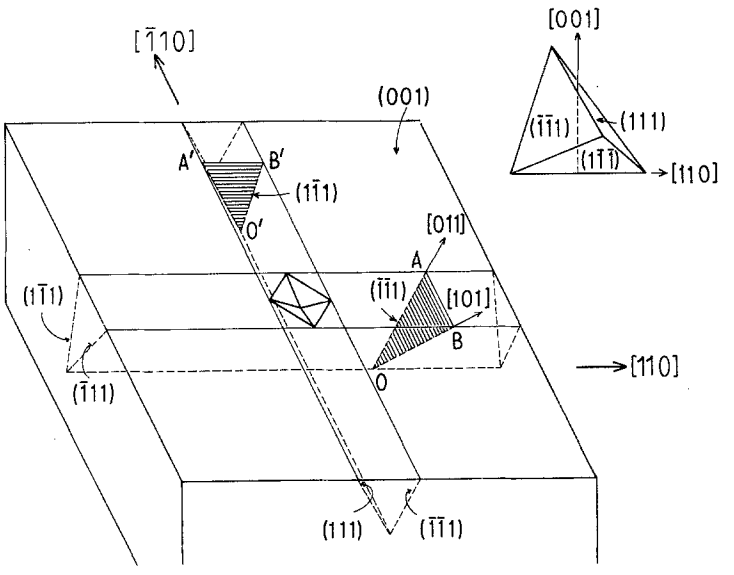

Figure 2 Simplified diagram of dislocation rosette configuration around an indentation on an {001} face of germanium. Prismatic dislocation loops such as AOB glide away from, and remove material (shaded) from, the indentation "plastic zone".

the indentation, partials of one type only are generated which then propagate along the slip plane. Further TEM studies are in progress so as to distinguish between these alternatives. These results should also be compared with those of Eremenko and Nikitenko [16], who performed TEM of indented silicon, and attributed a similar stacking fault contrast around the indentations to propagation of twins on {1 1 1} planes.

The dislocations move out from the indentation site under the influence of the stressfields produced by indentation. These stressfields have been analysed by several workers (e.g. [17, 18]), based on models involving a compact region of intense plastic deformation immediately below the indenter, surrounded by a region deformed purely elastically. Such stressfield models have been used to relate the lengths of rosette arms in silicon to the stresses on the dislocations [11]; such analyses are discussed in Section 4.

Fig. 4 shows the variation in rosette size with temperature and doping. Rosette size plotted is that interpolated to a standard 20 μm indentation size, so as to minimize differences in rosette size due to variations in hardness with doping. It can be seen that the data from each doping lie on widely separated curves, with the rosettes being consistently larger in the (ascending) order P, I, N (at room temperature, rudimentary rosettes could be seen around the indentations in n-type specimens only). This indicates that dislocations are more mobile in the n-type specimens than in intrinsic, and less mobile in p-type than in intrinsic. These results correlate well with those from dislocation velocity measurements on germanium [1, 12].

The rosette data from the specimens indented with a heated indenter, shown on the same diagram, show reasonable matching to the data from unheated-indenter experiment, bearing in mind that, in the cold-indenter experiments, the sizes of the indentations are characteristic of a lower temperature than those of the rosettes.

Note that the data for the three different dopings converge at 480 to 500° C. This is consistent with the convergence of data for microhardness (Section 3.1) and dislocation density measurements (Section 4.3). Such a convergence would be expected, as at these temperatures the intrinsic carrier concentration approaches that due to doping to the levels used here.

3.3. Median/radial crack lengths

Sharp indentations in brittle materials are often surrounded by cracking. The normal patterns of such cracks have been described by Lawn and Wilshaw [19], and can generally be classed into two types: those normal to the indented surface ("median" cracks and "radial" cracks), and those approximately parallel to the surface ("lateral" cracks). The lengths of median/radial cracks, as a function of indenting load, can be used to give information about the fracture toughness of the material (e.g. [20]).

Fig. 5 shows the variation of crack length at 50 g load (total crack span visible on the surface)

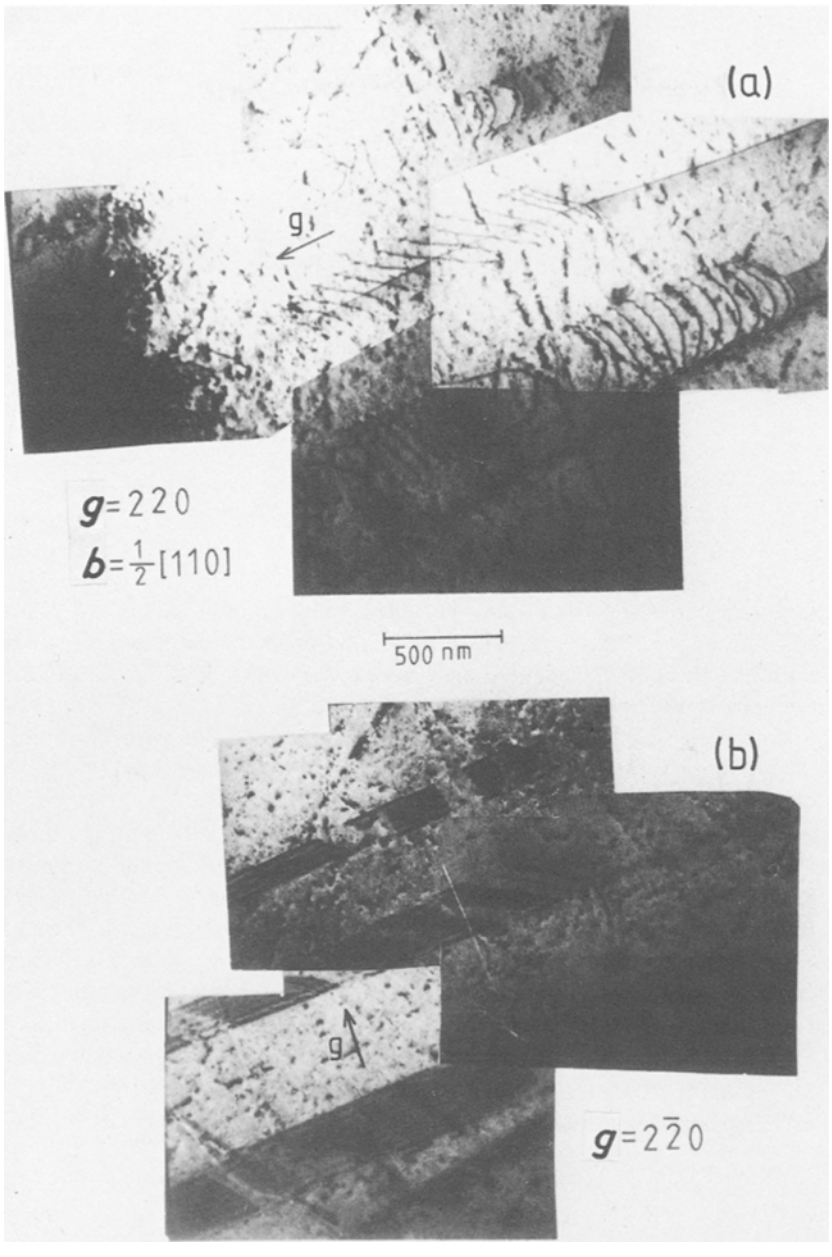

Figure 3 Transmission electron micrographs of one side of a rosette arm in intrinsic germanium (10 g indentation at 360° C). (a) Diffracting conditions show (partial) dislocations; (b) diffracting conditions show their associated stacking faults.

as a function of temperature and doping. It can be seen that at low temperatures, data from all specimens lie on the same line. As the testing temperature increases, the data curves for each doping diverge from this line, the cracks becoming rapidly shorter. This divergence occurs at a well-defined temperature for each doping: N, 290° C; I, 350° C; P, 400° C. Interpreted on the basis of models such as those of Lawn and Marshall [20], this would imply that, above a critical temperature dependent on doping, the fracture toughness (K_{Ic}) of germanium increases rapidly ($K_{Ic} \propto$ crack length$^{-3/2}$). However, these models assume a constant crack geometry (half-penny shape), so that the depth of the crack bears a constant relation to its span, regardless of size. This assumption was

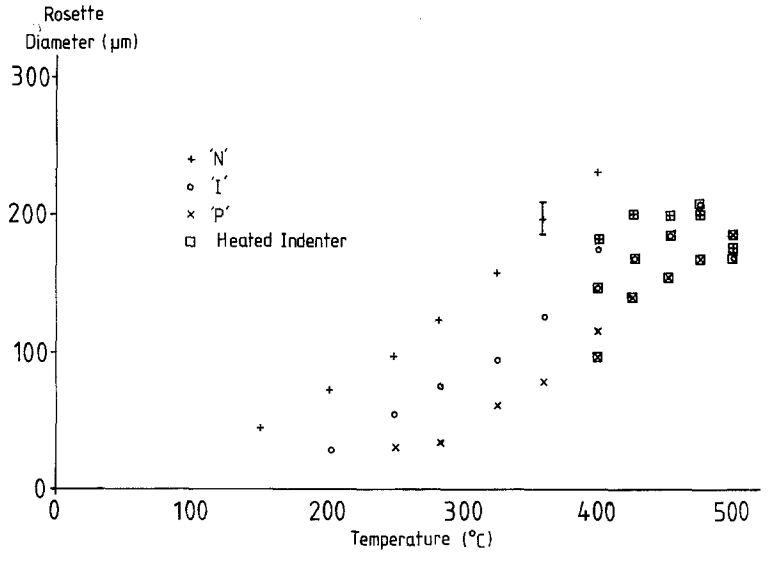

Figure 4 Variation in rosette size, normalized to a 20 μm indentation size, with doping and temperature. Note the strong dependence of rosette size on doping, with data for all dopings converging at ~ 500° C.

checked by making specimens with a line of closely spaced indentations across them, which were then broken along the line of indentations by bending. The cracks could then be examined in profile. Fig. 6 shows examples of such cracks; it can be seen that whereas the crack span as seen on the surface differs with doping above ~ 290° C, the depths of the cracks remains constant. Examination of the rosette structure shows that where cracks are shortened, they end in the heavily dislocated zone near the centre of the rosette, whereas cracks of "normal" length end in apparently dislocation-free material. The near-surface ("radial") cracks are believed to form on unloading the indenter [20]. It therefore seems that the shortening of the near-surface part of the cracks is due to interactions between dislocations produced in the loading stage of indentation and the parts of the crack which appear on unloading. Such indentations might be of two types:

1. Reduction of the crack-opening stress (from the indentation stressfield) by the stresses from the dislocation array.

2. Increase of the energy needed for crack extension, by work done in moving dislocations near the crack tip.

The deep part of the crack ("median" crack) is not affected by the relatively shallow dislocation structures in the rosette; in any case, these cracks are believed to form on loading the indenter, and might therefore be expected to have propagated ahead of any dislocations.

In the specimens indented in the hot-hardness

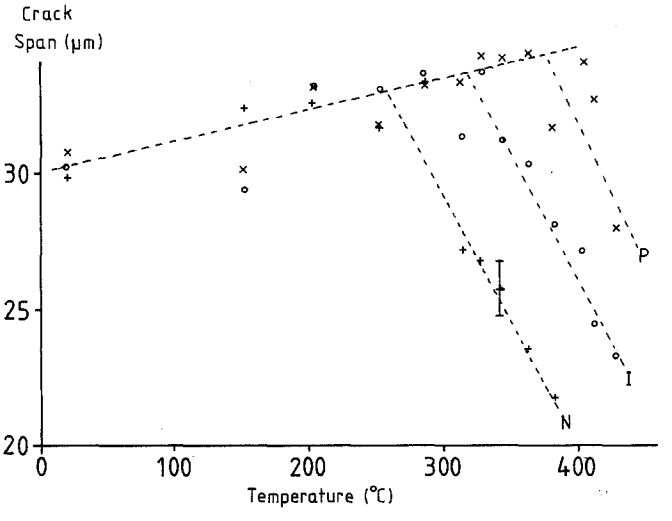

Figure 5 Variation in crack size (total span as measured on the surface) with temperature and doping, for 50 g load. The data from each doping diverge from a common line at a distinctive "ductile/brittle transition temperature", varying at ~ ± 50° C from intrinsic with doping.

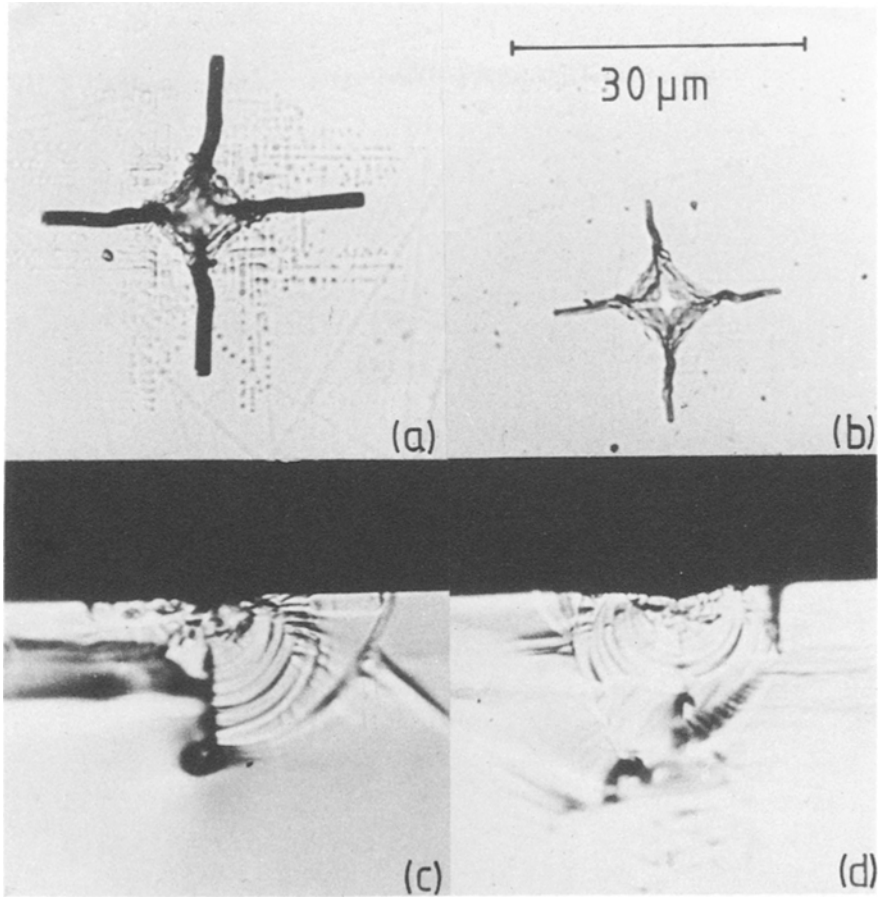

Figure 6 Crack geometry around 50 g indentations in p-type (a, c) and n-type (b, d) germanium at 360° C, seen in plan (a, b) and cross-section (c, d). Note that though the surface ("radial") crack size depends on doping, the crack depth ("median" crack size) does not.

tester at Cambridge (using a heated indenter), median/radial cracks were seen only around the p-type specimen indented at the lowest temperature (400° C). No cracks were seen around indentations in p-type material at higher temperatures, or around n-type or intrinsic material at any temperature in the range 400 to 500° C. Crack profiles such as those in Fig. 6 suggest that a minimum size of crack, associated with the propagation of the median crack alone, should be visible at the surface. It therefore appears likely that as well as the brittle/ductile transition temperature associated with radial crack propagation through dislocated material, there exists a higher brittle/ductile transition temperature related to the nucleation and/or propagation of the median cracks. Further experiments are in progress to investigate these effects and their dependence on doping.

4. Modelling and analysis of rosette data

This section contains a summary of some approaches to the analysis of rosette data. A more complete discussion of the relations between dislocation mobility, indentation hardness and rosette size will be presented in a further paper.

4.1. Models based on indentation stress fields

Attempts were made to apply the model previously used for rosette data from silicon [11] to the data from germanium. This model calculates the stresses on dislocations from the indentation stress field (as analysed in [17, 18]) and the dislocation interactions; a value of a minimum stress for dislocation motion (τ_{crit}) is derived. This approach was not successful in the analysis of the germanium data, in that the wide variation in the rosette sizes shown in Fig. 4 gave rise to only

very small differences in the calculated values of τ_{crit}. The failure of this type of model is attributable to the relaxation of the indentation stress field by the motions of the dislocations in the rosette arms; the indentation stress-field models [17, 18] assume that only elastic deformation occurs outside the region immediately under the indenter. In silicon, the relaxation is less important, since the rosettes are relatively short and contain few dislocations, all of which lie within the region within which the indentation stress field is strong compared with dislocation interaction stresses.

4.2. Measurement of dislocation positions

The method used was that due to Hu [21]. Here, dislocation positions are measured, the dislocation interaction stresses calculated, and the form of the indentation stress-field (assumed to be an inverse-power-law of distance from the indentation) derived by curve fitting. Hu found that, for rosettes in silicon at 700 to 900° C, the form of the stress-field could be uniquely derived from the data, and thus a well defined value of τ_{crit} could be calculated. This was not the case for the data from measurement of dislocation positions in germanium; almost any form of stress-field fitted the data equally well, allowing a wide range of values of τ_{crit} to be derived. This may be because the dislocation densities at the rosette arm ends were still high enough to allow even small errors in measuring the positions of the centres of etch pits to make unique curve fitting impossible.

4.3. Dislocation density measurements

The separation of dislocation etch pits at the ends of rosette arms allowed dislocation densities to be calculated. If it is assumed that at the ends of rosette arms, the residual stresses from the indentation centre are effectively zero (because of the distance from the indentation centre, and the relaxation of the stresses by the motion of dislocations in the "elastic" region), then the stresses from dislocation interactions should be the only significant ones acting; "order-of-magnitude" calculations based on stress-field models such as [17] and [18] show this to be the case.

Measurement of dislocation densities at rosette arm ends (see Table II) showed that, at a given temperature, the densities increased in the (ascending) order N, I, P. As the temperature increased, the differences between the dislocation densities at the ends of the rosette arms of the differently doped specimens decreased; at 500° C there was effectively no difference between them. At 425° C, the dislocation density at the rosette arm ends in the n-type specimen was less than half that in the p-type specimen. Since the dislocation spacings were assessed over a distance large compared to the mean spacing and since the dislocation densities in the rosette arms increase only slowly as the indentation is approached, it is reasonable to assume that these differences in dislocation spacings reflect differences in the friction stress. A simple calculation, integrating the forces on the outermost dislocation from all the others in the same rosette arm, assuming a constant dislocation density in the arm, gives a "lower bound" value for the stress on this dislocation numerically equal to ~ 20 MPa × (number of dislocations per micron), i.e. in the range ~ 6 to 30 MPa, depending on doping and temperature in the range 310 to 475° C. Such values, although relying on very crude approximations, do at least seem to be of the right order of magnitude, compared to the critical resolved shear stresses for slip in four-point bend tests [12].

TABLE II Dislocation densities at rosette arm ends

Temp. (°C)	Type	Dislocation spacing (μm)	Standard deviation (μm)	1/Spacing (μm^{-1})
475	P	2.9	0.5	0.34
	I	3.0	0.8	0.33
	N	2.9	0.3	0.34
450	P	2.1	0.3	0.48
	I	2.7	0.7	0.38
	N	3.2	0.6	0.31
425	P	1.3	0.1	0.77
	I	2.0	0.3	0.50
	N	2.8	0.6	0.36
400	P	1.5	0.4	0.66
	I	2.0	0.3	0.50
	N	2.4	0.2	0.41
360	P	1.1	0.2	0.91
	I	1.3	0.2	0.77
	N	2.0	0.3	0.50
310	P	–	–	–
	I	0.7	0.2	1.40
	N	1.2	0.3	0.83

5. Conclusions

Indentation experiments on doped germanium

crystals have shown that:

1. In the temperature range ~ 300 to 500° C, microhardness varies with doping. Heavily doped p- and n-type specimens are respectively harder and softer than intrinsic. The biggest variation with doping is at ~ 400° C; above and below this temperature, data from the different dopings converge.

2. TEM examination of indented specimens indicates that the dislocations in the rosette arms are of the Shockley partial type. These dislocations could be either dissociated "normal" dislocations, with the stacking fault width being much larger than the equilibrium value, or a series of partial dislocations all with the same Burgers vector.

3. Over the temperature range studied (20 to 500° C), indentation dislocation rosette size depends strongly on doping. Rosettes in p-type and n-type material are respectively smaller and larger than in intrinsic. The data from the three dopings converge at ~ 500° C.

4. Dislocation densities at rosette arms ends vary with doping, and reflect differences in the friction stress opposing dislocation motion. The densities can be used to estimate a lower-bound stress on the outermost dislocation; this stress falls in the range ~ 6 to 30 MPa, depending on doping and temperature. The differences in dislocation densities between dopings decreases steadily with increasing temperature in the range 310 to 475° C; at the highest temperature, data from the different dopings are not distinguishable.

5. The fracture behaviour of germanium varies with doping. The temperature at which radial cracks shorten with increasing temperature varies by ~ ± 50° C from that for intrinsic material (350° C). This "ductile/brittle transition temperature" is highest for p-type germanium, lowest for n-type germanium. These changes in the crack length are effective at the surface only, and do not change the crack depth.

6. The variations in mechanical properties with doping noted above are consistent with the known variation of dislocation velocity with doping in germanium. The convergence of hardness and rosette-based results at ~ 500° C is consistent with the fact that at this temperature, the intrinsic carrier density approaches that due to doping to the levels used in these experiments.

Acknowledgements

The work reported in this paper was supported by the SERC and by the Venture Research Unit of BP plc. The hot-hardness experiments using a heated indenter were carried out with the help of Dr T. F. Page, of the Department of Metallurgy and Materials Science, University of Cambridge, whose assistance is gratefully acknowledged.

References

1. J. R. PATEL and A. R. CHAUDHURI, *Phys. Rev.* **143** (1966) 601.
2. J. R. PATEL and P. E. FREELAND, *Phys. Rev. Lett.* **18** (1967) 833.
3. A. GEORGE and G. CHAMPIER, *Phys. Status Solidi* **53a** (1979) 529.
4. H. L. FRISCH and J. R. PATEL, *Phys. Rev. Lett.* **18** (1967) 784.
5. P. HAASEN, *Phys. Status Solidi* **28a** (1975) 145.
6. P. B. HIRSCH, *J. Physique Colloque* **40** (1979) C6-117.
7. R. JONES, *Phil. Mag.* **42B** (1980) 213.
8. S. B. KULKARNI and W. S. WILLIAMS, *J. Appl. Phys* **47** (1976) 4318.
9. P. B. HIRSCH, in "Proceedings of the Symposium on Defects in Semiconductors", edited by J. Narayan and T. Y. Tan (Elsevier/North-Holland, 1981) p. 257.
10. J. RABIER, P. VEYSSIERE and J. L. DEMENET, *J. Physique Colloque* **44** (1983) C4-243.
11. S. G. ROBERTS, P. PIROUZ and P. B. HIRSCH, *ibid.* **44** (1983) C4-75.
12. P. PIROUZ and P. E. FREELAND, unpublished work (1983).
13. B. TUCK, *J. Mater. Sci.* **10** (1975) 321.
14. K. SUMINO and H. HASEGAWA, *Trans. Jpn. Inst. Metals* **9** (1968) 749.
15. K. WESSEL and H. ALEXANDER, *Phil. Mag.* **35** (1977) 1523.
16. V. G. EREMENKO and V. I. NIKITENKO, *Phys. Status Solidi* **14a** (1972) 317.
17. S. S. CHIANG, D. B. MARSHALL and A. G. EVANS, *J. Appl. Phys.* **53** (1982) 312.
18. E. H. YOFFE, *Phil. Mag.* **46A** (1982) 617.
19. B. R. LAWN and R. WILSHAW, *J. Mater. Sci.* **10** (1975) 1049.
20. B. R. LAWN and D. B. MARSHALL, *J. Amer. Ceram. Soc.* **62** (1979) 347.
21. S. M. HU, *Appl. Phys. Lett.* **31** (1977) 139.

Received 6 June
and accepted 6 July 1984